Geodetic Application of Satellite Altimetry

Wolfgang Bosch
Deutsches Geodätisches Forschungsinstitut, München, Germany.
bosch@dgfi.badw.de

Abstract. Satellite altimetry has developed to an operational remote sensing technique with important applications to many geosciences. In the present paper we consider in particular geodetic applications of satellite altimetry. It is shown that this space technique not only allows mapping and monitoring a major part of the Earth surface, but also did contribute to essential improvements for the Earth gravity field. Even with the new dedicated gravity field missions of CHAMP, GRACE and GOCE satellite altimetry will be needed for the determination of the high-resolution gravity field. The mean sea level can be mapped and monitored for seasonal and secular changes through the combination of altimeter mission with different space-time sampling. The realisation of the global mean sea surface will help to unify national height systems, to clarify local sea level trends visible in tide gauge records and contribute to studies on the global sea level rise, the most prominent indicator of global change.

Keywords. Satellite altimetry, mean sea surface, gravity anomalies, Earth gravity field, Geoid, height systems.

1 Introduction

Geodesy deals with the surveying and mapping of the figure of the Earth. This includes the determination of the Earth gravity field. Soon after the first artificial satellites geodesy developed and applied new, space based technologies that allowed to overcome the limitation of terrestrial measurements. Today, global navigation systems like GPS and GLONASS (later GALILEO) have become standard tools for precise point positioning and the precise orbit determination of low orbiting satellites used to monitor the Earth surface (e.g. satellites carrying altimeter sensors).

The last few decades satellite altimetry has developed to an operational remote sensing technique with extremely important application to Earth sciences. The precise, fast, and nearly global monitoring of the ocean surface is – of course – an essential source for any research on ocean dynamics. There is a similar impact of satellite altimetry to geodesy. This technique contributes essentially to the solution of fundamental geodetic problems: mapping of the figure of the Earth, determination of the Earth gravity field, unification of height systems, and information about the rotation and orientation of the Earth. The altimeter mission history (See Fig. 1) provides a considerable number of missions with different orbit configuration and sampling characteristics that support many geodetic applications. The present keynote tries to give an overview to geodetic application of satellite altimetry.

2 Mapping of the Sea Surface

More than two third of the Earth surface is covered by oceans. A technique that allows to precisely map the ocean surface thus contributes essentially to the determination of the figure of the Earth. In the following a few details are described to understand the way that satellite altimetry is used to map the sea surface.

2.1 The Space-Time Sampling

A dedicated processing with precise orbit determination and a careful correction of the radar measurement for geophysical effects allows to deduce sea surface heights along the sub satellite track with a repetition rate of about one second (for details of this pre-processing we refer to Chelton et al. 2001).

Due to the average speed of the altimeter satellite the along track sea surface heights are separated by about seven km. The spatial resolution of altimetry, however, is limited by the spacing of neighbouring subsatellite tracks. This spacing in turn is governed by the orbit, configured for most missions such that the subsatellite track is repeated after a fixed number of days, the so-called repeat cycle. Unfortunately, orbit dynamics does not allow to fulfil both, a high spatial resolution and a short repeat cycle. TOPEX/Poseidon repeats its ground tracks every 9.9156 days – the spacing of tracks at the equator, however, is 2.8°, about 310 km (see Fig. 2).

International Association of Geodesy Symposia, Vol. 126
C Hwang, CK Shum, JC Li (eds.), International Workshop on Satellite Altimetry

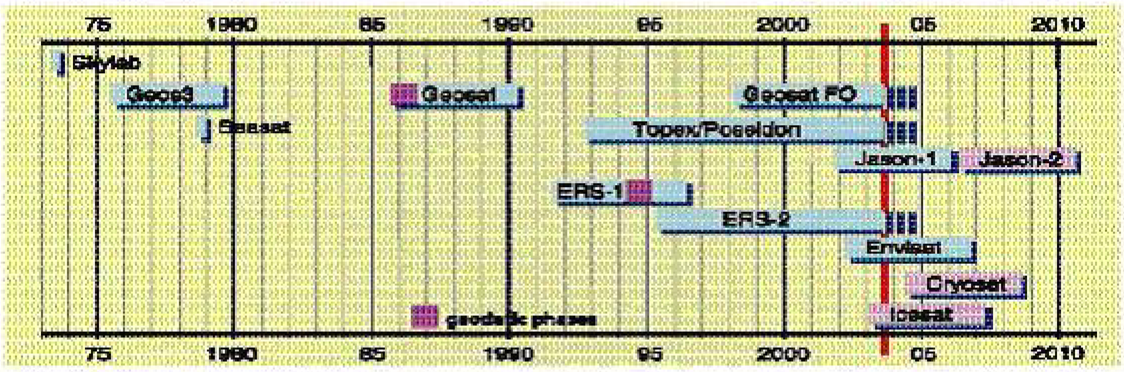

Fig. 1 Altimeter mission history

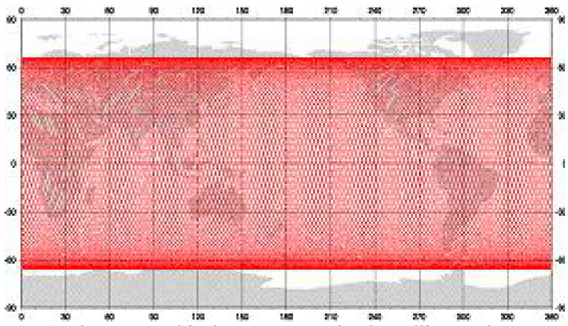

Fig. 2 The geographical coverage and subsatellite track pattern of TOPEX/Poseidon

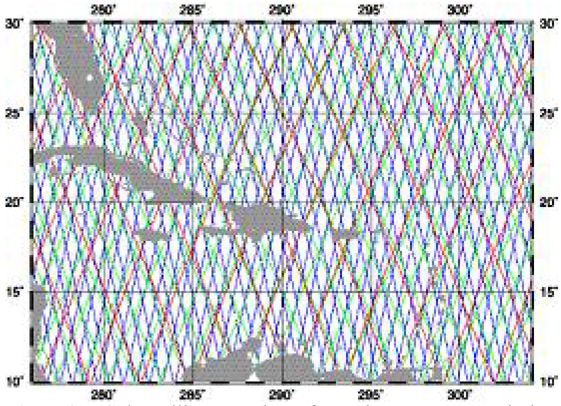

Fig. 3 Subsatellite tracks for the repeat missions TOPEX/Poseidon, ERS-1/2 (35 day) and Geosat/GFO in the area of the Caribbean Sea

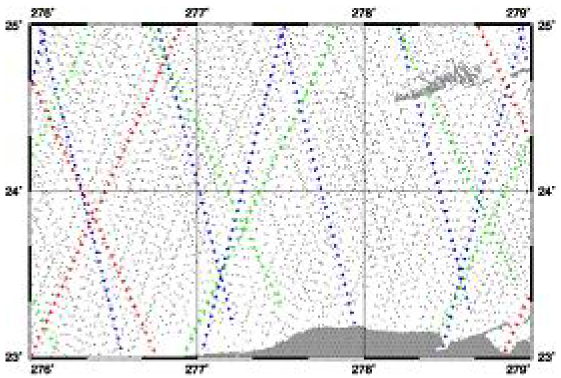

Fig. 4 A 2°x3° sub area showing not only measurements of the repeat missions but also the sampling due to the non-repeat geodetic missions of ERS-1 and Geosat.

The ground tracks of the 35-day repeat cycles of ERS-1/2 are separated by only 80 km. The spatial sampling of Geosat and GFO, both with a 17-day repeat cycle, is in between (165 km track separation). Fig. 3 demonstrates the improved spatial resolution that can be achieved by the combination of altimeter missions with different repeat orbit configurations.

An even better spatial resolution was obtained by the Geosat geodetic mission (GM) and the geodetic phase of ERS-1 with two 168-day repeat cycles. Fig. 4 demonstrates the sea surface heights measurements of these geodetic missions for a small sub area of 2°x3°.

The radar measurement itself is *not* a point measurement but a mean value for the so-called footprint, that part of the sea surface from which reflected radar pulse were received. The size of this footprint depends on the instantaneous wave height and its radius varies between about 2-11km.

2.2 Mean Sea Surface Models

The mapping of the sea surface is the most obvious geodetic application. In particular the geodetic missions provide a spatial resolution that allows to estimate mean sea surface heights on a 2’x2’ grid. Most of the mean sea surface height models developed in the last decade are listed in Table 1.

For the two most recent models, CLS01 and GSFC00.1, we summarize the slightly different processing strategies. Hernandez and Schaeffer (2001) basically applied a statistical approach to

Table 1. Global models of the mean sea surface – possibly incomplete results of the last decade

Model	Missions	Latitude	Resolution	Reference
MSS93A	Geosat, ERS-1	80°S-80°N		Anzenhofer & Gruber (1995)
MSS95A	TOPEX/Poseidon, ERS-1	80°S-80°N	3’x3’	Anzenhofer et al. (1996)
OSU-MSS	TOPEX/Poseidon, ERS-1, Geosat			Yi (1995)
MSS GRGS	TOPEX/Poseidon, ERS-1	80°S-80°N	3,75’x3,75’	Cazenave et al. (1996)
CSR98	TOPEX/Poseidon, ERS-1/2, Geosat	82°S-80°N		http://www.csr.utexas.edu/ocean/
CLS_SHOM98	TOPEX/Poseidon, ERS-1, Geosat	80°S-82°N	3,75’x3,75	Hernandez et al. (1998)
CLS_SHOM98.2	TOPEX/Poseidon, ERS-1/2, Geosat	80°S-82°N	3,75’x3,75’	Le Traon et al. (1998)
KMS99_MSS	TOPEX/Poseidon, ERS-1, Geosat	82°S-82°N	3,75’x3,75’	Anderson & Knudsen (1998)
GSFC00.1	TOPEX/Poseidon, ERS-1/2, Geosat	80°S-80°N	2’x2’	Wang (2001)
CLS01	TOPEX/Poseidon, ERS-1/2, Geosat	80°S-82°N	2’x2’	Hernandez & Schaeffer (2001)

determine CLS01:

1. Multi-mission altimeter data (CORSSH), as harmonized by CLS AVISO
2. ERS-1 data corrected from ocean variability by “optimal analysis”
3. Sea level anomalies referenced to TOPEX/-Poseidon mean profiles for the period 1993-2000
4. Least square collocation for a 2’ grid with error covariances for altimetry and ocean variability noise and along-track biases

For land areas, CLS01 was augmented by the EGM96 geoid and smoothed in a transition zone from land to sea. For the GSFC00.1 model (Wang 2001) a more deterministic approach was applied:

1. Harmonization of multi-mission altimeter data (Pathfinder Projekt, Koblinsky et al., 1999)
2. Sea surface height profiles of all missions averaged to mean tracks.
3. Non-TOPEX/Poseidon missions adjusted to six years of TOPEX/Poseidon (cycles 011 - 232)
4. Sea surface height difference used for geodetic phases of Geosat and ERS-1.
5. Least squares adjustment of two-dimensional Fourier series in 2°x2° cells.
6. Fourier series evaluated for the 2’x2’ grid.

Note, both models were based on a careful harmonisation of data and took special care on the way to relate the geodetic mission data to the long-term average of TOPEX/Poseidon. Fig. 5 illustrates the small-scale features of the mean sea surface resolved by CLS01.

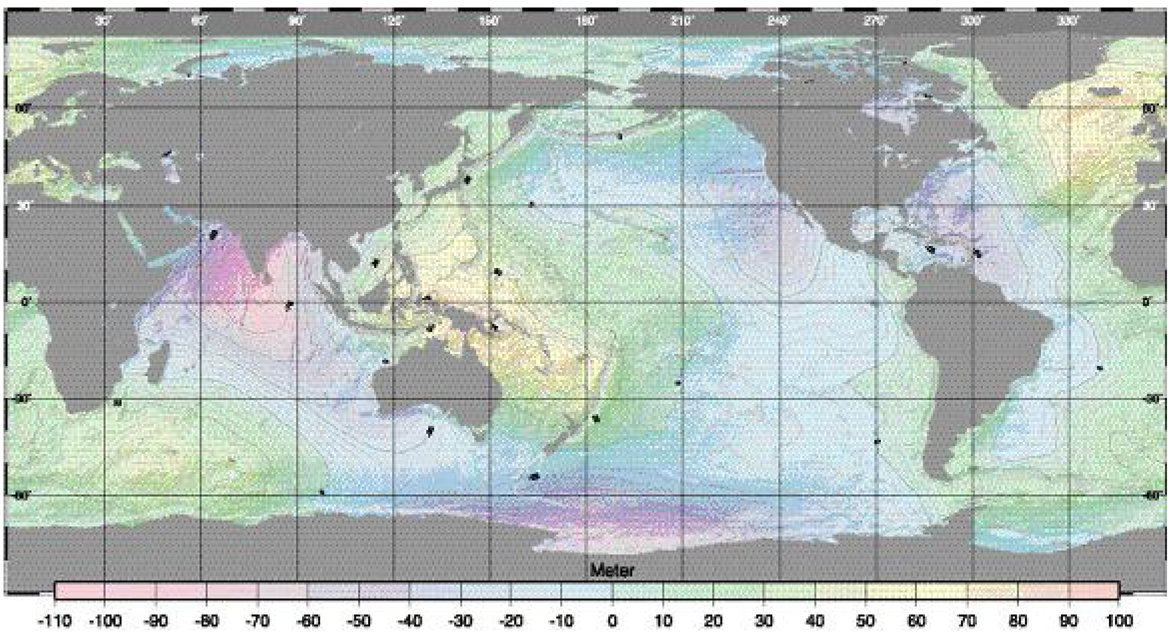

Fig. 5 The Mean sea surface model CLS01 (Hernandez & Schaeffer, 2001), generated from a combination of the TOPEX/Poseidon, ERS-1 and ERS-2 altimeter missions. The resolution of 2’x2’ allows to identify small-scale features of the sea surface that are caused by gravity variations of trench areas, fracture zones and mounts at the sea floor.

Even though these mean sea surface models achieve an astonishing resolution there are a few aspects that should be kept in mind:

- Mean sea surface models are based on different data periods and are representative only for these periods.
- There are large scale, low frequency changes of MSL in the order of 15-20 cm for time periods of 7-8 years (see below, Fig. 9)
- The global MSL appears to rise by 1-2mm/year
- Altimeter missions neither provide global coverage (TOPEX/Poseidon) nor miss long-term stability (ERS-1/2)
- There are large uncertainties for the inverse barometer correction. GSFC00.1 and CLS01, for example have a mean offset of 2-3 cm, mainly due to a different handling of the inverse barometer correction.

2.3 Seasonal Variation of the Sea Surface

In general, the sea surface is subject to changes on a wide range of spatial and temporal scales. For geodetic applications small scale and high frequency changes are, however, less important. Therefore we focus on seasonal and secular variations on global scale that may have impact to periodic or long-term variations of the Earth gravity field, its centre of gravity, and the Earth rotation.

The seasonal variation of solar radiation causes a rather fast heating and cooling of the upper layer water masses down to about 200m (the so called thermocline). This effect lets the sea surface fall or rise and is most efficiently described by harmonic analysis with an annual base period and some higher harmonics to account for a seasonal modulation of the annual wave. The sea surface height variations dh_{ik} at node k and time t_i may be modelled by

$$dh_{ik} = d_k \cdot \Delta t_i + \sum_{p=1}^{2} A_{pk} \cos(\omega_p \Delta t_i - \Phi_{pk}) \qquad (1)$$

where $\Delta t_i = t_i - t_{ref}$ is the time difference to some reference epoch t_{ref}, d_k is an additional drift term to account for secular changes, A_{pk} and Φ_{pk} are amplitudes and phases of period p at node k respectively and the angular velocity ω_p may be set to

$$\omega_p = \frac{2\pi}{T_p}, \quad \text{with } \mathrm{T}_1 = 365.25, \mathrm{T}_2 = 182.625, ... \qquad (2)$$

The geographical distribution of amplitudes and phases for the most dominant annual period *p=1* is shown in Fig. 6. It is clearly visible from the phases that there is an oscillation between northern and southern hemisphere although phase shifts are present in a small band between 10° and 20° northern latitude. Also the pattern of the phases in the Indian ocean deviates from a simple hemispheric distribution. The amplitudes show highest values at the strong western boundary currents, namely the Kuroshio and the Gulf Stream area. On average amplitude values in the southern ocean are smaller.

Because ocean surface currents are dominated by lateral stratified water movements (e.g. westward propagating Rossby waves), zonal mean values of sea surface heights may be in addition used to characterize the temporal variation of the global sea level. Fig. 7 shows the zonal mean values versus time.

2.4 Secular Sea Level Change

Global sea level rise is taken as the most prominent indicator of global change. Satellite altimetry appears to be predestinated to give an answer for the actual amount and possible acceleration of sea level rise. However, even after a few decades of altimeter missions, a sufficient long record with reliable long-term stability is still a problem. TOPEX/Poseidon just completed a decade of observation with the most precise orbit and ionospheric corrections from the two frequency altimeter sensor, allowing an in-situ estimation of the total electron content TEC (Imel 1994).

The bias of TOPEX/Poseidon is continuously controlled using overflights over the Harvest oil platform (Christensen et al. 1994). Drifts for the oscillator and the onboard radiometer were detected and taken into account. This all justifies to use the TOPEX/Poseidon time series for an estimate of global sea level change.

Fig. 8 shows the global mean as a function of time. The mean values were performed by weighting with cosine of latitude to account for the metric of the sphere. The annual oscillation is remarkable and not fully understood. The high latitude areas above/below 66° are not at all observed by TOPEX/Poseidon. Other components of the global water cycle (atmosphere, snow cover, or soil moisture) may at least partly compensate the

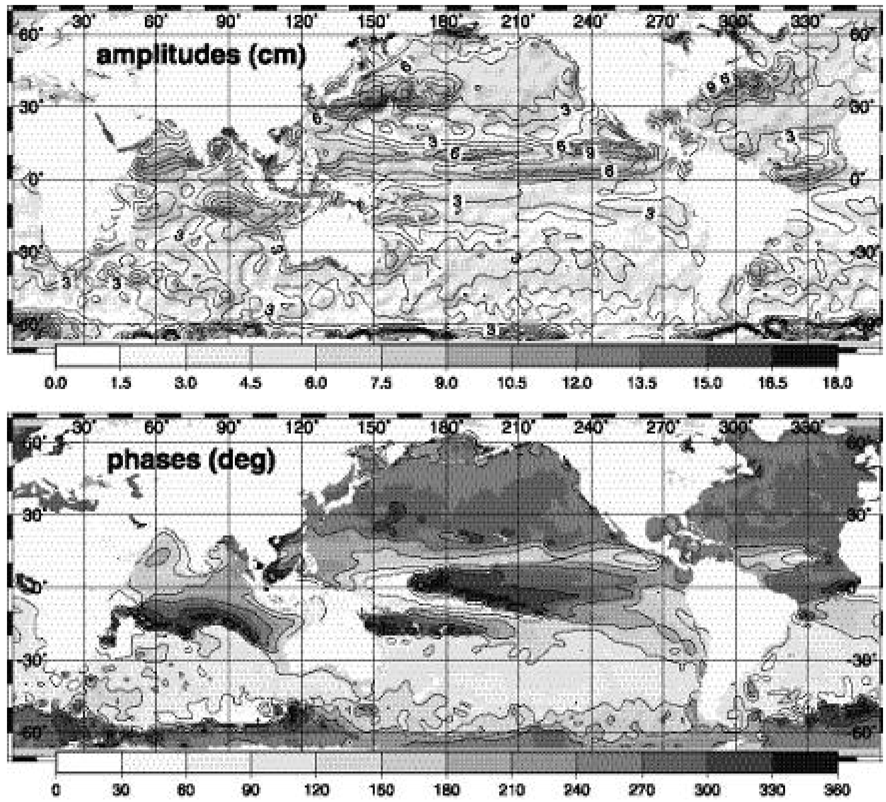

Fig. 6 Mean annual variation of the sea surface. The upper panel shows amplitudes (cm), the lower panel the phases (deg), relative to Januar 1. Amplitudes and phases below –55° are unreliable due to temporal sea ice coverage.

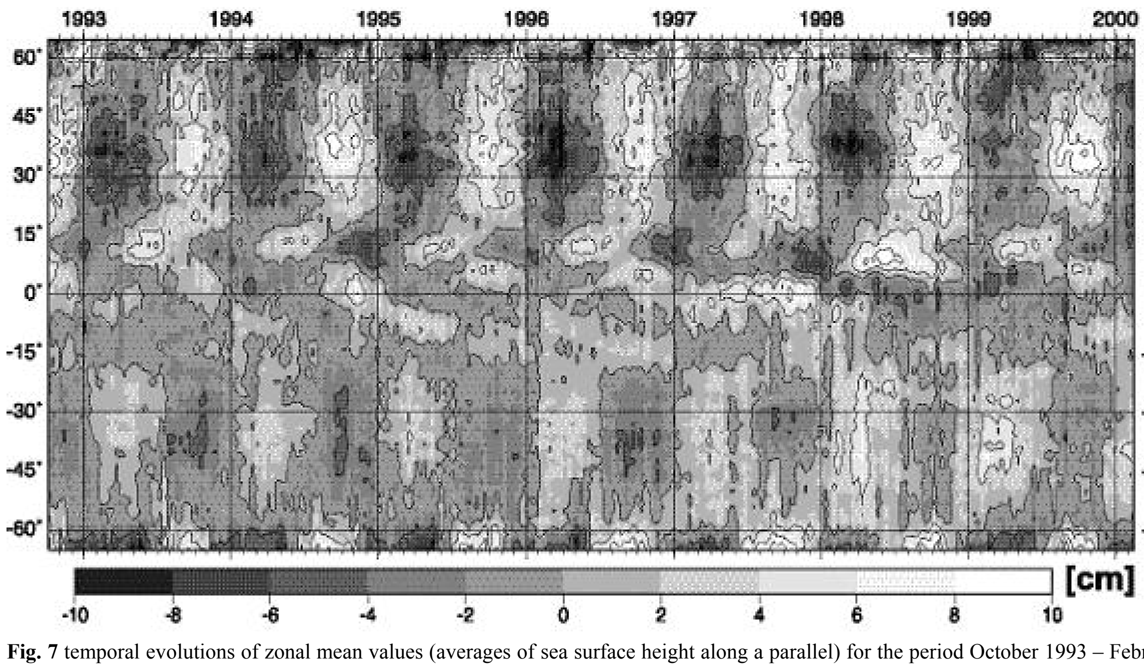

Fig. 7 temporal evolutions of zonal mean values (averages of sea surface height along a parallel) for the period October 1993 – February 2000 derived from TOPEX/Poseidon data. The strong El Niño end of 1997 is mapped to the anomalous high average sea level (white colour) at latitude 0°. The following La Niña effect with low sea level at the equator and relative high sea level at about 10° North and in the South Pacific is also seen during the year 1998.

annual oscillation observed for the global mean sea level. The drift of +1.9 mm/year is in agreement with other investigations.

It should be emphasized, however, that the secular evolution of the mean sea level is by no way uniform. Fig. 9 shows that there are large geographical pattern with a opposing sign for the mean rate of change. In the central Pacific the sea level has fallen by as much as 12 cm. In the Indonesian Seas there is a strong sea level rise of more than 15 cm for an eight years period.

It is far beyond this keynote to discuss the causes of the observed sea level changes. There is some agreement that the dominant part of the observed changes are caused by increased heat storage and the thermal expansion of the upper layer water masses.

3. Determination of the Earth gravity field

The mean sea level approximates the geoid, that particular equi-potential surface of the Earth gravity field that should serve as global height reference surface. In the early days of satellite altimetry the nearly coincidence of sea level and geoid was used to improve the knowledge about the geoid which suffered twenty years ago from errors in the order of 10 m. Today, the sea level can be determined with a few cm accuracy. At the same time, the gravity field (and thus the geoid) has been considerably improved - in particular through altimetry as will be indicated in section 3.2. However, our present-day knowledge of the gravity field is still insufficient to define a cm-geoid or to fulfil oceanographic requirements (see below).

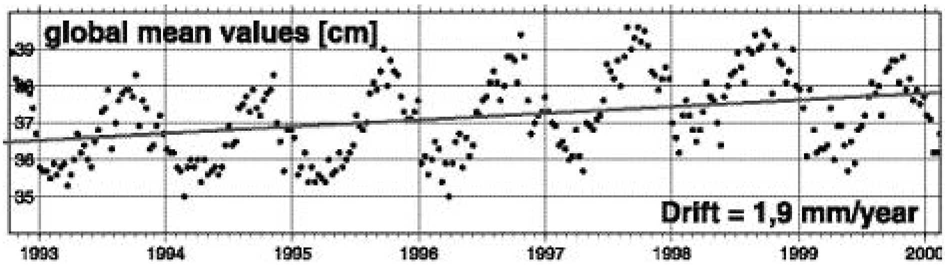

Fig. 8 Global mean value of sea level for the period 1993-2000, derived from TOPEX/Poseidon data.

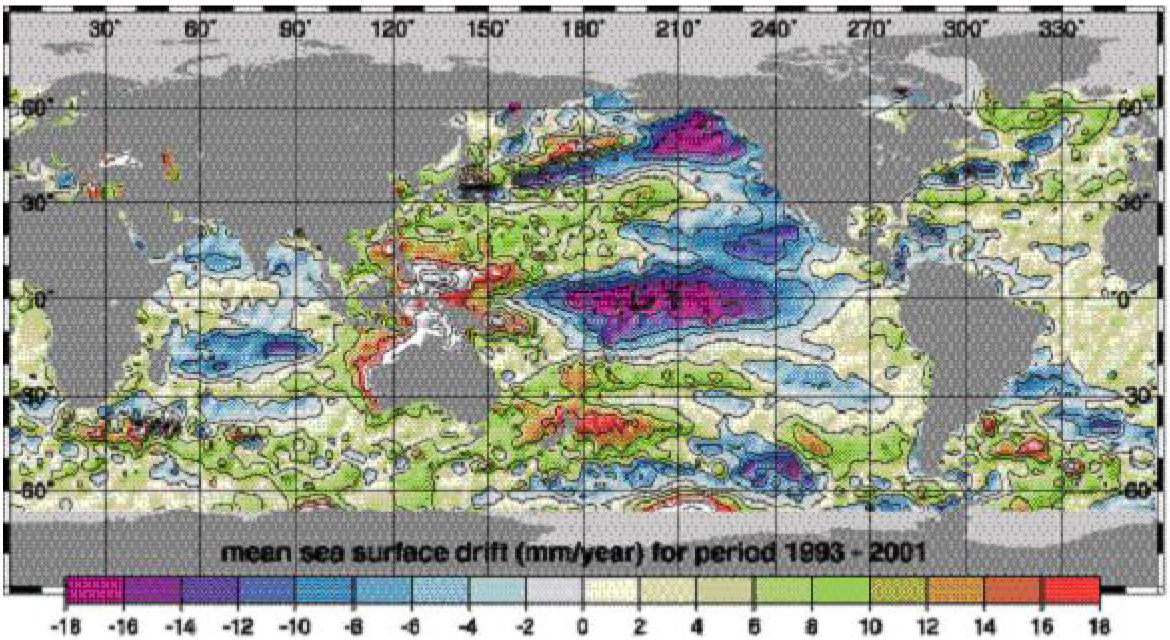

Fig. 9 Mean annual rate of change (mm/year) for the mean sea surface, estimated from TOPEX/Poseidon data for the period 1993-2001. In the central Pacific sea level fell by more than 11 cm. In the Indonesian Seas there is a sea level rise by more than 15cm.

3.1 From the sea surface to the geoid

It is well known that the mean sea surface is not coinciding with an equi-potential surface of the Earth gravity field. The deviation, called sea surface topography (SSTop) is caused by hydrodynamic processes. The SSTop is small in magnitude (only up to 2 m) but important for both, oceanography and geodesy.

Oceanography considers the SSTop as a signal, because it carries the signature of the ocean surface currents. For geodesy, SSTop may be considered as a disturbance. If the ocean would be in rest and in equilibrium with the gravity force only, the mean sea surface would realize the global height reference surface, geodesist are looking for in order to connect height systems on different continents. Long time there were mutual expectation what discipline should provide a reliable and precise estimate of the SSTop.

The geodetic attempts to estimate the SSTop are either based on a pure geometric approach (sea surface minus geoid) or were performed in a dynamic way, solving simultaneously for the gravity field and the SSTop. Both methods, however, are limited by the errors of the gravity field. In the open ocean, the state-of-the-art gravity fields, like EGM96 (Lemoine et al. 1998), still havegeoid errors of a few decimetres. This is neither sufficient to transform height datums from one continent to the other nor to estimate the two meter SSTop with a sufficient signal to noise ratio. Figure10 shows an estimate of the SSTop. It gives a qualitative correct view of the very large-scale structure of the SSTop dominated by subtropical and sub polar gyres in the ocean basins and strong western boundary currents. In order to derive reliable information about the surface currents and mass transports the slopes of the SSTop must be known, however, to a much higher precision.

The hydrostatic and geostrophic equilibrium may be crude approximations of the equation of motion. But for most areas of the ocean they are able to give a quantitative right picture of the dominant part of the general flow. Considerable progress has been also achieved for the numerical modelling of ocean currents. These models integrate the Navier-Stokes differential equation and are driven by actual wind and pressure fields, assimilate altimeter data and provide a resolution down to ¼ of a degree. The "Parallel Ocean Climate Model" POCM (Semtner and Chervin, 1992) and ECCO, "Estimation of the Circulation and Climate of the Ocean" (Stammer et al. 2003) are examples for sophisticated and expensive numerical modelling efforts.

With the present limitations of the geoid it is therefore reasonable to use the altimetric sea surface and subtract the dynamic topography as obtained from oceanographic modelling in order to get an improved geoid. Wunsch and Stammer (2003) currently argue this way.

Both, the geodetic and the oceanographic community are looking forward to dramatic geoid improvements that are expected from the dedicated gravity field missions CHAMP, GRACE and GOCE. Once, a cm-geoid has been achieved the geodetic approach may again become a valid procedure that allows to deduce many details of the surface currents. On the long term, however, the

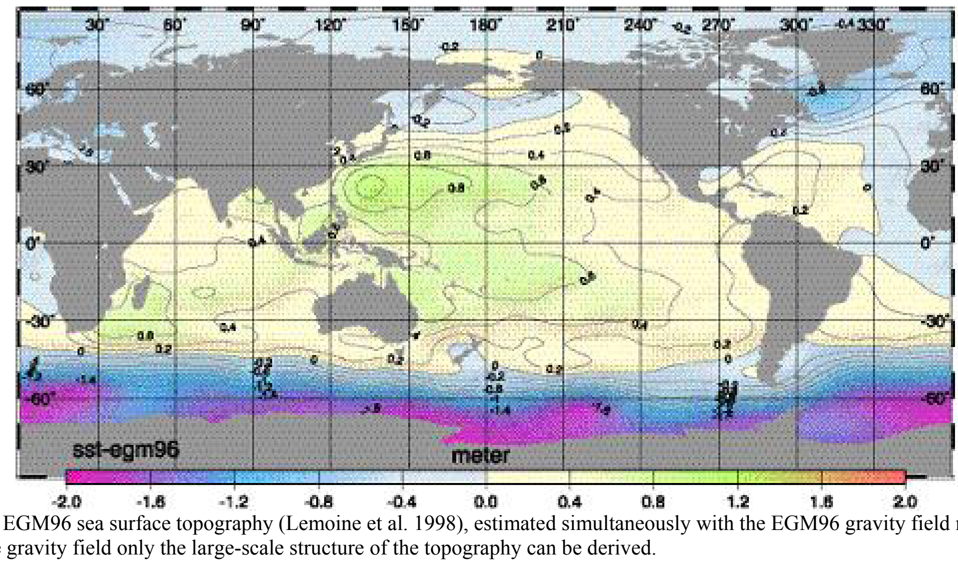

Fig. 10 The EGM96 sea surface topography (Lemoine et al. 1998), estimated simultaneously with the EGM96 gravity field model. Due to errors of the gravity field only the large-scale structure of the topography can be derived.

determination of the surface currents and the improvements of the geoid must be considered as a common estimation problem (Wunsch and Stammer 2003).

3.2 Marine gravity anomalies

How did altimetry contribute to gravity field improvements of the last decade? It is worth, to review this contribution, because altimetry will keep its role even, if there are essential improvements through the new gravity missions. It is conservative to assume that altimetry is able to map the mean sea surface with a spatial resolution of 5'x5' (the most recent models go down to 2'x2'). A 5'x5'-resolution corresponds to a harmonic degree beyond 2000! The gravity field models of GOCE will not go beyond degree 300. Thus the high frequency information of the marine gravity field will be further based on satellite altimetry.

The recovery of marine gravity anomalies is founded on famous geometry - gravity relationships, expressed by the Stokes and Vening Meinesz formulas (Heiskanen and Moritz, 1967)

$$N = \frac{R}{4\pi G}\iint_{\sigma} \Delta g S(\psi) d\sigma \qquad (3)$$

$$\begin{Bmatrix} \xi \\ \eta \end{Bmatrix} = \frac{1}{4\pi G}\iint_{\sigma} \Delta g \frac{ds}{d\psi} \begin{Bmatrix} \cos\alpha \\ \sin\alpha \end{Bmatrix} d\sigma \qquad (4)$$

$S(\psi)$ is the Stokes function, G gravity and the unit sphere. The inversion of these formulas allows deriving gravity anomalies Δg either from the geoid or from the slopes ξ, η of the geoid, the deflections of the vertical. The inversion can be realized either by a Fast Fourier Transform (FFT) or by Least Squares Collocation (LSC) technique. For global applications both methods are one by one applied to a sequence of local areas in order to avoid - in case of LSC - the inversion of huge matrices or to ensure the validity of the planar approximation in case of FFT. To localize the inversion, a remove-restore technique is applied, generating in advance residual quantities by subtracting a state-of-the art gravity field like EGM96. After inversion the gravity anomalies of this reference field are restored.

The estimation of gravity anomalies from satellite altimetry was first demonstrated with Seasat data by Haxby et al. (1983). Numerous applications followed: McAdoo and Marks (1992a, 1992b) Sandwell and Smith (1997), Hwang and Parsons (1998) and Anderson et al. (2000, 2001). Global maps, as shown in Fig. 11 demonstrate the high resolution of gravity anomalies from multi-mission satellite altimetry, using in particular the geodetic phases of Geosat and ERS-1.

The data processing has been continuously improved by updated altimeter corrections, outlier detection, filtering and retracking of the altimeter data. In particular in polar areas with temporal coverage of sea ice a dedicated signal analysis is required to recover gravity anomalies (Laxon and McAdoo, 1994).

A general problem in recovery anomalies from the geodetic missions is that the level of neighbouring profiles, measured at different epochs is considerably affected by sea level variability. The required slope information is thus corrupted by the sea level variation and would be transformed to noisy gravity anomalies if not special care is taken to account for the sea level variability.

Thus, crossover adjustments and low-pass filtering, proven methods, which are applied, for the mapping of the mean sea surface are also required for the recovery of marine gravity. Indeed, a high-resolution mean sea surface can be considered as essential step towards the estimation of gravity anomalies. For example, gravity anomalies and vertical components of the gravity gradient were computed from GSFC00.1 (Wang 2001) by numerical evaluation of the inverse Stokes integral. Also, the multi-mission processing of Anderson et al. (2001) result in both, a mean sea surface and a detailed map of marine gravity anomalies.

3.3 High resolution gravity field modelling

Gravity field models derived only by rigorous least squares adjustment of satellite tracking data (so called satellite-only gravity fields) are limited in resolution, up to about degree and order 70. There are several reasons: Either high-orbiting satellites are insensitive to small scale anomalies of the gravity field or the orbits of low satellites is disturbed by non-gravitational forces like atmospheric pressure or difficult to estimate with only ground based tracking systems.

The high-resolution marine and terrestrial gravity data can improve the situation. However, the combination of terrestrial gravity and satellite-only gravity field models is a computational problem. Solving by least squares the coefficients of a harmonic series up to degree and order 360 implies to invert a system with 130321 unknowns.

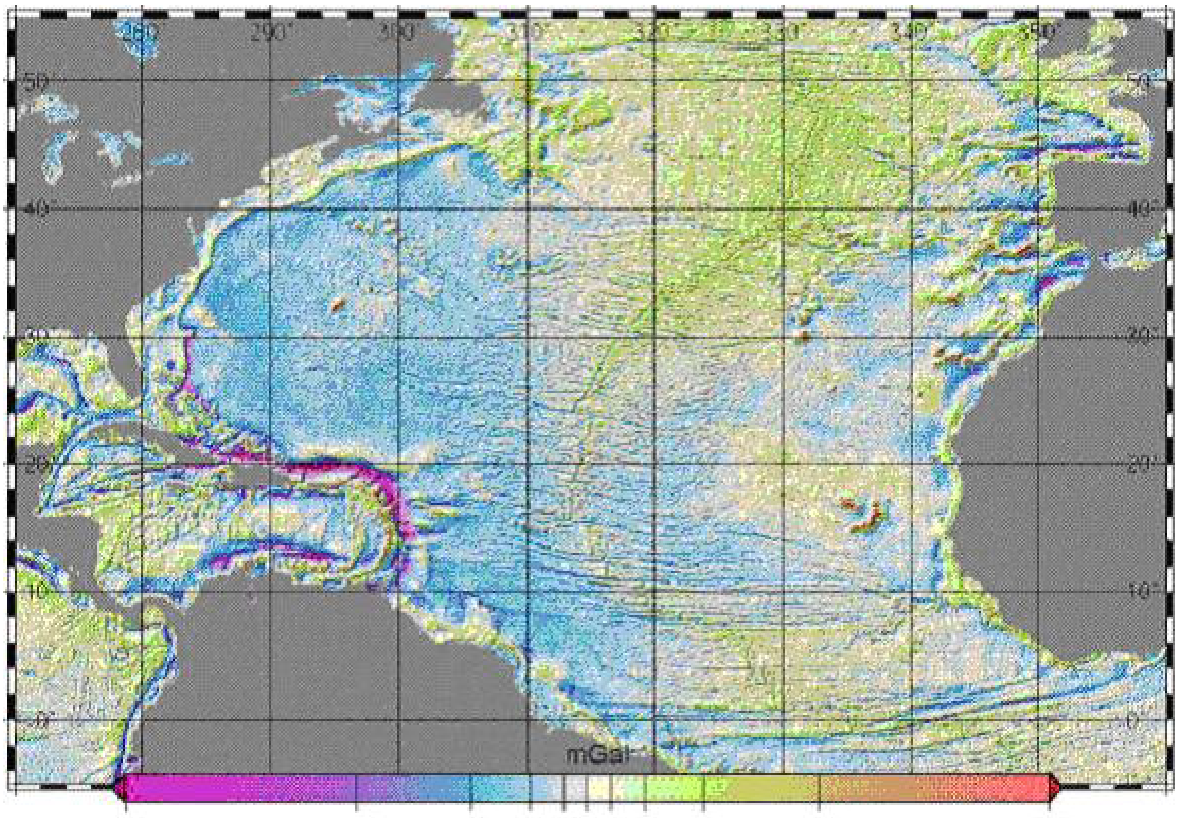

Fig. 11 Marine gravity anomalies [mGal] in the North Atlantic reflect details of the Puerto-Rico trench area, the mid-Atlantic ridge and many fracture zones. (Version 9.2 anomalies generated globally by Sandwell and Smith, 1997)

Bosch (1993) showed that the normal equation degenerate to a block diagonal structure, if the surface data

1. is organized in latitude bands with equidistant spacing,
2. is complete (global coverage, no gaps), and
3. has homogeneous weights within the latitude bands not depending on longitude.

The diagonal blocks of the matrix have decreasing size, starting from the desired maximum degree and order. (See Fig. 12) Such a block-diagonal matrix is easy to invert. Even the combination with the normal equation of a satellite-only field is solvable if the unknown are arranged in a particular way. This combination strategy with a reverse sequence of unknown as proposed by Schuh (1996) has been applied for the EGM96 gravity field (Lemoine et al. 1998) extended up to degree and order 360.

The essential step was the construction of a complete, homogeneous set of 30'x30' surface data combining terrestrial and marine gravity anomalies, the latter derived from satellite altimetry. Later on this data set has also been used for the GRIM5-C1 gravity model (Gruber et al. 2000) a brut-force combination with full normal equation matrices for satellite-only and terrestrial gravity data complete to degree and order 120. The rigorous combination of terrestrial gravity data with new gravity fields from CHAMP, GRACE and GOCE remains an open issue.

3.4 Gravity gradients

Another simple geometry - gravity relationship is based on the Laplace Equation and Bruns formula (Rummel and Haagmanns 1991). The disturbing potential T fulfils

$$T_{zz} = -(T_{xx} + T_{yy}) \tag{5}$$

With Bruns formula this can be transformed to

$$T_{zz} = -2J\gamma \tag{6}$$

showing that the gravity gradients can be derived from the mean curvature J of the geoid. Instead of the geoid the mean sea surface may be used, because offsets between geoid and the sea surface have no impact and even the slopes of the SSTop do not corrupt the value of *J*.

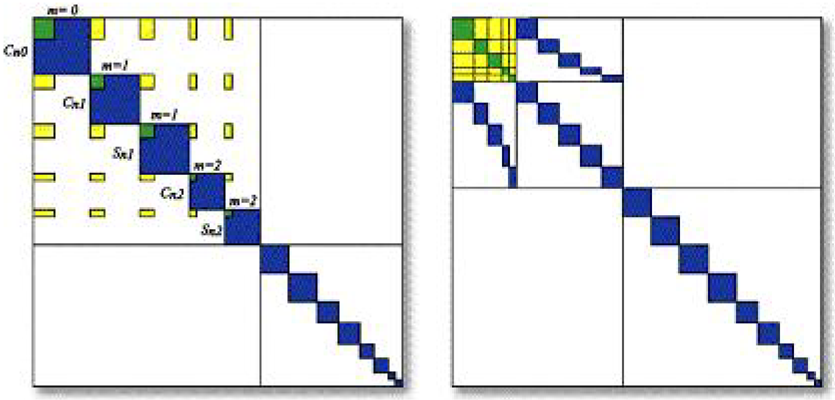

Fig. 12 Structure of normals for a least squares estimate of spherical harmonics combining surface gravity (dark blue) and satellite-only normal equations (yellow). Left hand: All unknowns are arranged primary with respect to order. The re-arrangement of unknowns (right hand) with the satellite-only normals, kept together, is easier to solve.

4 Single- and Dual-Satellite Crossovers

Whenever two subsatellite tracks cross each other it is possible to compare the sea surface heights derived from both tracks. For example, ascending and descending tracks of a single satellite have one and only one *single-satellite crossover* (see Fig. 13). Two subsatellite tracks of different missions may perform none, one or two *dual-satellite crossovers*, depending on the different orbit configurations, in particular the different inclinations of the orbital plane.

The power of using crossovers is based on the fact that they provide redundancy: the sea surface height at the crossover location can be derived twice - by interpolating the sequence of measurements along both intersecting tracks.

This interpolation is required because in general there is no direct measurement at the intersection of the two ground tracks. In addition the computation of crossovers is laborious because every ascending track may intersect all descending tracks – but only intersection over ocean can be used. The strategy to compute crossover differences therefore first approximates the crossover location, then verifies if the location is over ocean and finally performs the interpolation only if there are enough and high quality measurements close to the crossover event.

The difference of sea surface heights at the crossover location is then

$$\Delta x_{jk} = h_j^{sat} - \left(r_j^{alt} + \sum_n corr_n^j \right) - h_k^{sat} + \left(r_k^{alt} + \sum_n corr_n^k \right) \tag{7}$$

where h^{sat} is the height of the satellite above a reference ellipsoid, r^{alt} the altimeter based range measurement and $corr_n$ a number of necessary environmental corrections to be applied to the altimeter range. If the two measurement *j* and *k* are taken nearly simultaneously or with a short time difference of less than a few days, the crossover differences Δx_{jk} do *not* reflect by sea level changes but can be attributed to orbit errors or errors of the environmental corrections that were applied to the altimeter measurements.

4.1 Crossover Statistic, a Measure of Quality

The accuracy of sea surface heights may be characterized by an error budget with individual error estimates for all components of the altimeter systems (see for example table 11, page 120 in Chelton et al., 2001). A statistic of crossovers, computed with a short time delay, may be used as well to characterize the overall error budget.

AVISO (1999) report, for example, the history of the global mean of TOPEX/Poseidon single-satellite crossovers, performed for every cycle. On average the mean crossover standard deviation is about 7 cm, which includes not only orbit errors but also all errors of the environmental corrections.

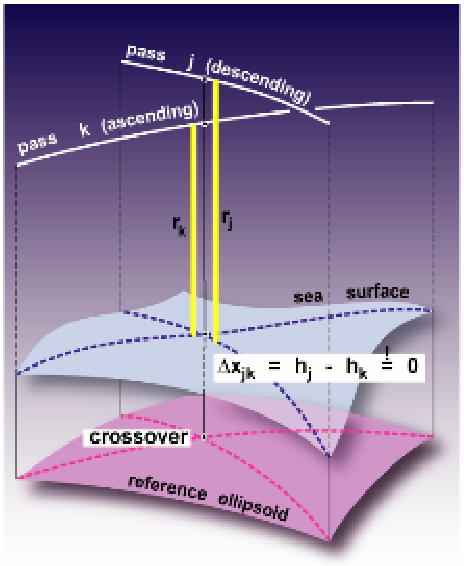

Fig. 13 Crossover scenario with redundant sea surface height measurements

4.2 Orbit Error Estimates

The redundancy of crossover differences can be used to estimate correction for the radial component of altimeter systems. In the early days of altimetry, orbit errors were the dominant error source for the radial component. Consequently, crossover differences Δx_{jk} have been used for a least squares estimate of orbit errors δo_{jk} by observation equations of this form

$$\Delta x_{jk} + v_{jk} = \delta o_j - \delta o_k \tag{8}$$

where the subscripts j and k indicate independent orbit error models for the two intersecting tracks.

Different models were used to express the orbit error. For crossover analysis within a limited region a simple "tilt&bias" model may be sufficient to represent the orbit error, which is known to be of long wavelength structure. For larger areas, polynomials have been used; for global analysis trigonometric functions, splines or piecewise cubic polynomials with C^1 continuity conditions were applied to avoid any discontinuity in the estimated orbit errors. Schrama (1989) gives a comprehensive discussion on orbit errors estimated by crossover adjustment. Shum et al. (1990) developed a procedure for the direct use of crossovers in the precise orbit determination.

Dual-satellite crossovers provide additional capabilities to improve the radial component of altimeter systems. Above all, this has been used for those altimeter missions that could not achieve the same orbit accuracy as TOPEX/Poseidon. Long time, the orbit accuracy of TOPEX/Poseidon (about 2-3 cm for the radial component) was exceptionally. This was mainly due to the rather high mean altitude of 1336 km, reducing the effect of non-gravitational forces, which are difficult to model. Moreover, the TOPEX/Poseidon orbit could be determined by laser, GPS and DORIS. The microwave systems GPS and DORIS realize a nearly continuous tracking and allow to compute so called "reduced dynamic" orbits, which are rather independent of gravity field errors (Yunck et al. 1994).

For ERS-1, flying at an altitude of about 800 km, the orbit determination was much more difficult. After the early failure of the PRARE tracking system only laser tracking data was available such that the errors of the radial component of ERS-1 was about two or three times higher than for TOPEX/Poseidon.

The use of dual-satellite crossover between TOPEX/Poseidon and the ERS satellites solved the problem. It was reasonable to keep the orbit of TOPEX/Poseidon fixed and to estimate radial corrections to improve the orbits of ERS-1 and ERS-2 (Le Traon and Ogor, 1998). This demonstrated that dual-satellite crossovers are an efficient tool to construct a vertically consistent series of sea level measurement from altimeter missions with different sampling characteristic.

4.3 Validating and Tuning the Earth gravity field

Rosborough (1986) has shown that the radial orbit errors Δr for ascending passes (A) and descending passes (D) of a satellite i are composed of a "mean" part ($\Delta\gamma$) and a "variable" part ($\Delta\delta$) such that

$$\Delta r_i^A = \Delta\gamma_i + \Delta\delta_i \tag{9}$$

$$\Delta r_i^D = \Delta\gamma_i - \Delta\delta_i \tag{10}$$

Based on Kaulas theory (1966) both orbit error components, the mean and the variable part, can be expressed as function of the errors $\delta C_{lm}, \delta S_{lm}$ of the gravity field harmonics:

$$\Delta\gamma_i = \sum_{l,m} Q_{lm}^{Ci}(a,I,\phi)\cdot(\delta C_{lm}\cos m\lambda + \delta S_{lm}\sin m\lambda) \tag{11}$$

$$\Delta\delta_i = \sum_{l,m} Q_{lm}^{Ci}(a,I,\phi)\cdot(\delta C_{lm}\sin m\lambda - \delta S_{lm}\cos m\lambda) \tag{12}$$

The functions $Q_{lm}^{Ci}(a,I,\phi)$ depend on the semi-major axis a and the inclination I of the satellite and the geocentric latitude ϕ (for an efficient computation of these functions see Bosch, 1997) .

As long as there are no improved gravity field through the new gravity field missions it may be reasonable to assume that crossover differences mainly reflect orbit errors induced by an insufficient modelling of the Earth gravity field. Fig. 14 shows a long-term average of ERS-1 single-satellite crossover differences. The geographical pattern is due to errors of the JGM3 gravity field, which was used to compute the ERS-1 orbits.

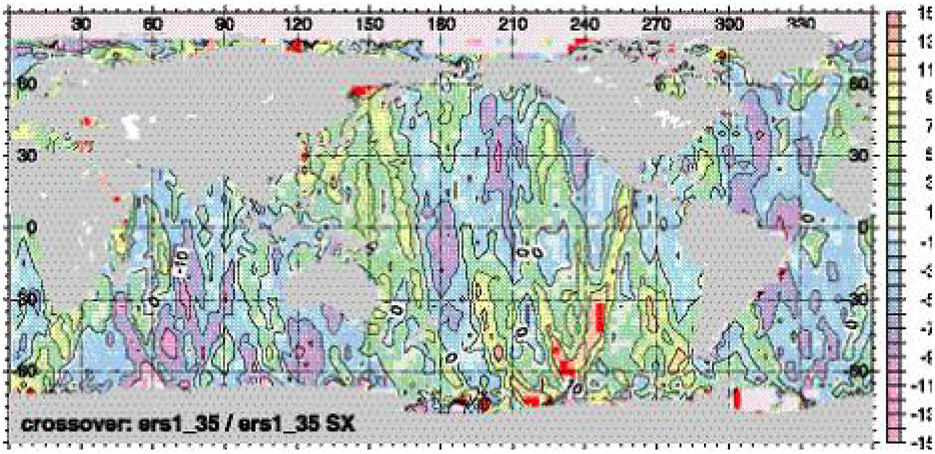

Fig. 14 An example for a pronounced geographical pattern of mean single-satellite crossover differences, computed for ERS-1 (35 day repeat) with JGM-3 orbits. Units are cm. The Atlantic and Indian Ocean have negative means while the South and West Pacific have positive means. The patterns are modulated by the subsatellite tracks of ERS-1.

Using the theory of Kaula and Rosborough, "observed" single-satellite crossover difference Δx_{ij} may be modelled by

$$\begin{aligned}\Delta x_{ij} &= \Delta r_i^A - \Delta r_j^D = 2\cdot\Delta\delta_i \\ &= 2\cdot\sum_{l,m} Q_{lm}^{Si}(a,I,\phi)\cdot(\delta C_{lm}\sin m\lambda - \delta S_{lm}\cos m\lambda)\end{aligned} \tag{13}$$

showing that the differences can be expressed as a function of errors of the gravity field harmonics. Similar equations can be set up for dual-satellite crossovers (see Klokocnik and Wagner, 1999). In single satellite crossovers the mean part $\Delta\gamma_i$ is cancelled. This error component, also called geographically correlated error, may only be visible in dual-satellite crossovers.

Both, single- and dual-satellite crossover differences have been intensively used by Klokočnik et al. (1996, 1999) for accuracy assessments of gravity field models.

The relationship between crossovers and harmonic coefficients was used by Scharroo and Visser (1998) to tailor the JGM3 gravity field by minimizing crossover differences between TOPEX/Poseidon and ERS-1 through an adjustment of harmonic coefficients. The tailored field, called DEGM04, reduces the root mean square orbit accuracy for the ERS satellites from 7 to 5 cm.

4.4 Reference System Offsets

Crossover residuals carry not only the signature of geopotentially based orbit errors but they also exhibit geographical pattern that are inconsistent with orbit dynamics. The satellite motion is described in an inertial system: the origin of the coordinate system is the centre-of-gravity and the moments of inertia for the x- and y-axes vanish. In order to have no centre-of-gravity offset all first degree harmonics must be zero. If the z-axis coincides with the axis of maximum inertia the harmonics of degree 2 and order 1 will also vanish.

These terms are called *forbidden harmonics*. Different tracking systems and tracking station distribution or week calibration conditions, however, may cause differences in the orbital reference frame system.

For both, ascending and descending tracks, an offset *dr* and coordinate shifts *dx,dy,dz* map into the radial direction by

$$\Delta\rho = dr \\ \quad - \cos\phi\cos\lambda dx - \cos\phi\sin\lambda dy - \sin\phi dz \tag{14}$$

For single-satellite crossovers offset and coordinate shift cancel each other and are not visible. Only dual-satellite crossover contain the differential effect of datum transformation for different satellites. They may be used to estimate offsets and shift parameters. However, datum parameters can only be estimated *for all but one* satellite. Any attempt to estimate datum parameters for all satellites would generate a singular system, because arbitrary large datum shifts, applied to *all* satellites would have no impact on the crossover differences. TOPEX/Poseidon has the most reliable orbit (as explained above). Therefore datum parameters are estimated only for *other* satellites and they describe datum differences *relative* to TOPEX/Poseidon.

Long-term averaged dual satellite crossover residuals among Geosat, ERS-1 and TOPEX/Poseidon, all with JGM3 based orbits, have been used by Wagner et al. 1997 and Bosch et al. 2000 to solve simultaneously for corrections to the gravity field harmonics and parameters accounting for a coordinate frame offset relative to TOPEX/Poseidon. The result showed significant offsets between the coordinate frames of the altimeter missions involved, but also large correlation between offset parameters and uneven degree, order one harmonic coefficients (see Fig. 15).

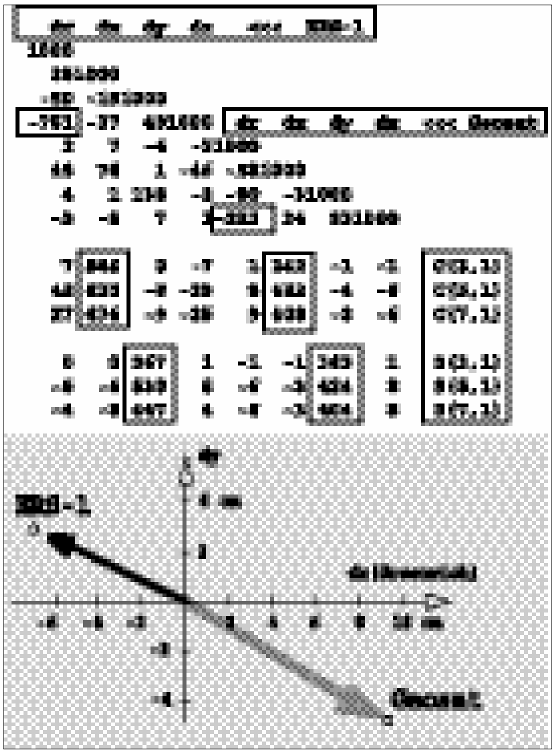

Fig. 15 Geocentre offsets estimated relative to TOPEX/Poseidon for ERS-1 and Geosat with a subset of the correlation matrix (scaled by the factor 1000) showing large correlations between dr and dz, and between the x- and y-shifts and uneven degree, order one coefficients.

5. Unification of Height Systems

Geometric height differences are measured along the local plumb line, which is everywhere orthogonal to an equipotential surface of the Earth gravity field. Therefore, an equipotential surface is the only proper height reference surface! On the other hand, the mean sea surface appears to be a "natural" reference for heights. For life at the coast and the coastal zone economy, it is essential to know the height above sea level! The traditional way to define national height systems was also oriented at mean sea level: The long term records of a tide gauge were averaged and the height of a near-by marker was defined relative to this realization of mean sea level.

Because we know today, that the mean sea surface does not coincide with an equipotential surface, this classical definition implies that systematic differences are possible whenever two heights at the same point refer to different height systems. The unification of height systems has become a major problem – above all through the growing demands to determine physical heights by the combination of precise point positioning and evaluation of the geoid!

5.1 Geoid definition and Bursa's approach

The foundations for a global heights system are known since more than 130 years: Listing (1873) defined the geoid as that particular equipotential surface of the Earth gravity field, that best fits to mean sea level. Together with Gauss and Helmert he suggested using this as a global height reference surface.

Listings definition is, however, not pragmatic; it doesn't give any recipe how to realize this surface. Instead a number of questions arise:

1. What gravity field model shall be used to compute equipotential surfaces (EGM96, or any of the new models from CHAMP, GRACE or GOCE) ?
2. There are several realization of mean sea level, averaged over different time periods with individual grids and coverage. Which one should be used?
3. How to realize the "best fit" between mean sea surface and the equipotential surface (least squares, global minimization, along the coast or at height reference points only?)

The way of realization will be a matter of convention. However, satellite altimetry will be essential for the realization itself.

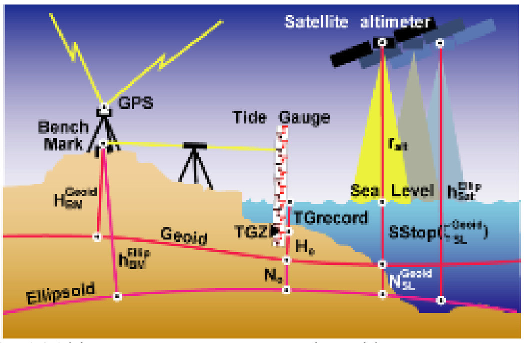

Fig. 16 Altimetry measurement scenario at tide gauges

Bursa et al. (1999, 2002) proposed to select the geoid by a geopotential value W_0 that should be derived as the mean of the geopotential W, evaluated over all ocean surfaces mapped by altimetry.

$$\int_{MSS} (W - W_0)^2 \, dMSS \rightarrow \text{minimum} \tag{15}$$

He uses the EGM96 gravity field and the sea surface heights of TOPEX/Poseidon as provided by AVISO (1998). Bursa argues that the value of W_0 is rather insensitive to changes in both, the gravity field and the sea surface heights – due to the global averaging. Bursa does, however, not account for long-term changes of mean sea level, shown in Fig. 9 above. The impact of these changes has to be investigated. It may be necessary to define the global height system for particular epochs.

5.2 SSTop estimated at tide gauges

Once, a geoid has been defined and the geopotential value W_0 is known, it will be necessary to estimate the offsets between geoid and height reference points of the national height systems. The principle appears to be simple. Precise positioning of the reference point gives geocentric coordinates, which are to be used to compute the geopotential value W_i at this point. Then

$$\delta H = \frac{1}{\gamma}(W_i - W_0) \tag{16}$$

gives the vertical offset between the national height system and the geoid. The problem here is that the errors of the gravity field corrupt the value W_i because for this step there is no averaging procedure!

Regional refinements of the geoid will be required to overcome the local errors of global gravity field models. Geopotential differences to neighbouring points, derived from levelling and gravity measurements, may be used to estimate the vertical offset to the geoid for other points on land as well. Over sea, a precise knowledge of the surface currents or equivalent the slopes of the SSTop can be converted to geopotential differences. A least squares minimization of all differences then allows deriving a best estimate of the offset between the geoid and the national height system.

5.3 Comparing sea level time series at tide gauges

Tide gauge measurements provide very precise records for the sea level if their reference level is regularly controlled by precise levelling. The problem is that tide gauges measure sea level relative to the solid Earth. Any vertical movement of the tide gauge site generates a trend in the recordings and may be interpreted as an apparent sea level rise or fall.

Since some time it is recognized that altimetry and tide gauges can complement and control each other (Neilan et al. 1998) in order to get a more reliable understanding of long term sea level changes. It was suggested to install and operate continuously operating GPS receivers at globally distributed tide gauge stations. The International GPS Service IGS initiated a pilot project TIGA (http://igscb.jpl.nasa.gov/projects/tiga/tiga.html) to estimate the vertical tectonic motions at these sites.

Satellite altimetry can be used to derive independent sea level time series at tide gauges. In most locations the temporal and spatial sampling of altimetry is by no way optimal. Also, the precision of altimetry is degraded near the coast (the footprint is still or already corrupted by land surface, there is a rapid change of environmental corrections). Nevertheless, points of the subsatellite track with closest approach to the tide gauge or with maximum correlation between sea surface height time series and tide gauge registrations have been used for relative comparisons. Within the Pathfinder project (Koblinsky et al. 1999a,b), but also within individual investigations (e.g. Acuña et al. 2002) the two time series showed up correlation factors up to 0.8 or even higher. Mitchum (1994, 1998) demonstrated that relative comparisons with 70 tide gauges can monitor the long-term stability of altimeter systems. The differences of both time series indicated instrumental drifts of –2.2mm/year. Later on, Mitchum (2000) presented an improved comparison taking into account land movements at the tide gauges.

Other investigations even perform *absolute* comparison. This is possible if the tide gauge zero point has been positioned in a geocentric system by GPS (See Fig. 16). The multi-mission sea surface heights must be related to the same reference system and can be extrapolated towards the tide gauge location. For example, subsatellite tracks from TOPEX/Poseidon and ERS-1 nearly hit the La Guaira tide gauge in Venezuela (see Fig. 17, Acuña and Bosch 2003, this volume). The mean heights of both time series are offset by only 3 cm, however, a significant trend of the differences is observed, that could not be explained.

Dong et al. 2002 perform an absolute calibration of TOPEX/Poseidon using six tide gauges in the UK. The bias of TOPEX is estimated with about ±2 cm precision, that of Poseidon with about ±3 cm.

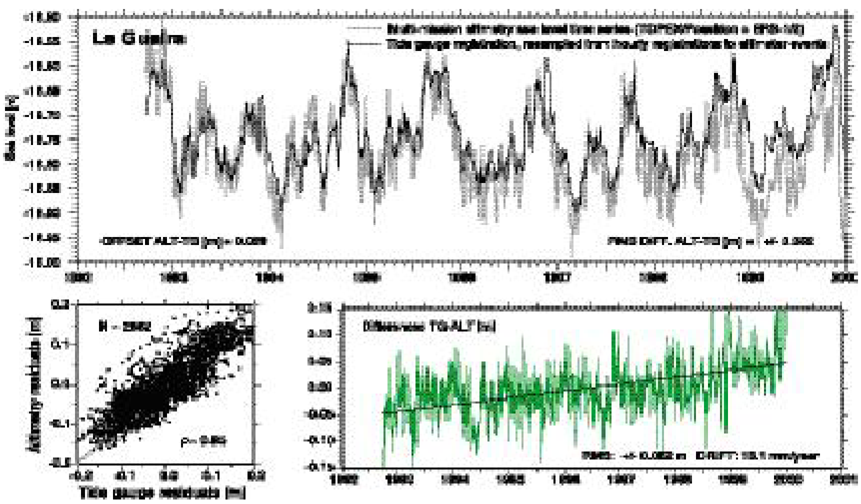

Fig. 17 Absolute comparison between tide gauge recordings and sea level time series from multi-mission altimetry (TOPEX/Poseidon + ERS-1/2).

6. Variation of low-degree harmonics

Satellite altimetry can help to estimate variation of low-degree gravity field harmonics induced by ocean mass redistribution. Because altimetry gives only *geometric* changes of sea level, additional information is needed to decompose mass- and volume change of ocean water. Once, this decomposition is known, the effect of the mass redistribution on the geocentre, the Earth rotation and gravity field is easily derived. This forward modelling may also contribute to a better understanding of the global water cycle.

Temperature and salinity determine water density. To estimate the thermohaline expansion of sea water, the so called steric effect, vertical density profiles must be known. Levitus (1994) compiled data of several decades and generated a climatology, the World Ocean Atlas WOA94, by objective analysis, WOA94 also provides monthly mean values of the dynamic heights which can be taken as a first guess for the annual variation of the steric effect. The differences between sea level variations and the variation of the steric effect gives an estimate of the mass redistribution.

6.1 Geocenter variations

Because of the very small mass variations the further computations can be performed in spherical approximation. Assuming a constant density ρ_w, the mass variations can be condensed to the sphere and described by the equivalent height changes. These heights can be expanded into spherical harmonics.

$$h(\theta,\lambda) = \sum_{n=0}\sum_{m=0} P_{nm}(\cos\theta)\cdot\left[a_{nm}\cos m\lambda + b_{nm}\sin m\lambda\right] \tag{17}$$

The harmonic series allows a simple evaluation of integrals using the orthogonality relations of spherical harmonics. The shifts of the geocentre is finally expressed as a function of the degree one coefficients of the harmonic series

$$\begin{Bmatrix}\Delta x\\ \Delta y\\ \Delta z\end{Bmatrix} = \frac{4\pi\rho_w R_E^3}{M_E\sqrt{3}}\begin{Bmatrix}a_{11}\\ b_{11}\\ a_{10}\end{Bmatrix} \tag{18}$$

where R_E and M_E are the mean radius and the mass of the Earth respectively. Fig. 18 shows geocenter shifts estimated from TOPEX/Poseidon minus Levitus monthly mean dynamic heights. Similar computations have been perfomed by Dong et al. 1997 and Chen et al. 1999.

With an amplitude of 3.5 mm the z-component in Fig. 18 shows the most dominant shifts. Shifts for x and y-axis show large deviations from an annual oscillation end of 1997. This is due to the strong El Niño which is –of course - not reflected in the mean dynamic heights of Levitus. Obviously, the multi-year averages of the climatologic data is not well suited to be compared with in-situ sea level changes observed by altimetry. A better source of information is expected to be provided by numerical models like ECCO (see Wunsch and Stammer 2002).

6.2 Second and higher degree harmonics

The redistribution of ocean masses also changes the angular momentum of the Earth and the higher degree and order coefficients of the Earth gravity field. Gross (2002) shows, for example, how the inertial tensor of the Earth depends on the second degree coefficients of the Earth gravity field.

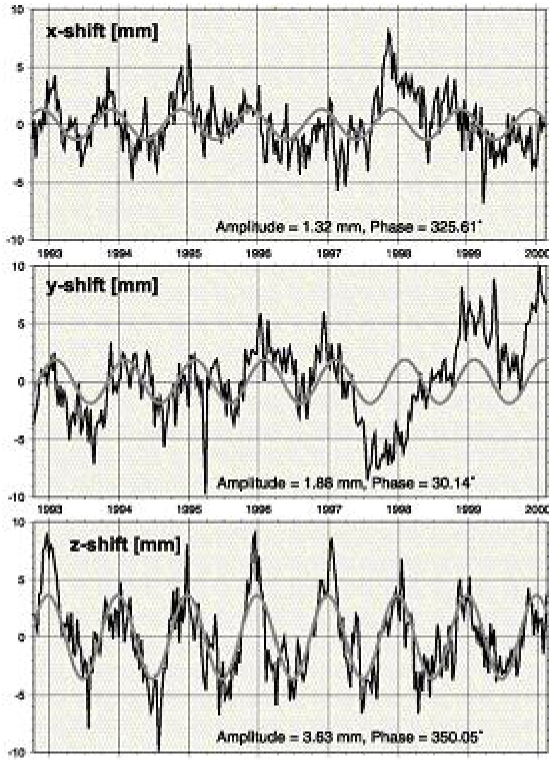

Fig. 18 Time series of geocenter shifts estimated from TOPEX/Poseidon minus Levitus (1994) monthly mean dynamic heights. The grey curve is a fit of an annual period with amplitudes and phases listed below.

The changes of second and higher degree coefficients of the Earth gravity field can be derived similar to the geocentre shifts. Indeed, Wahr et al. 1998 show that the ocean mass redistribution, condensed to a layer with density $\Delta\sigma = \rho_w \cdot h$ implies a change of the gravity field harmonics by

$$\begin{Bmatrix}\Delta C_{lm}\\ \Delta S_{lm}\end{Bmatrix} = \frac{3}{4\pi\bar{\rho}(2l+1)}\iint_s \Delta\sigma(\theta,\lambda)\cdot\bar{P}_{lm}(\cos\theta)\begin{Bmatrix}\cos m\lambda\\ \sin m\lambda\end{Bmatrix}dS \tag{19}$$

where ρ_w and $\bar{\rho}$ are water density and the average density of the Earth respectively, and $\bar{P}_{lm}$ are the normalized Legendre functions. In addition to the direct effect the surface masses also load and deform the solid Earth. This indirect effect can be accounted for by a factor $(1+k_l)$ where k_l are the load Love numbers for degree l.

7 Conclusions

7.1 Problems and Perspectives

Satellite altimetry has become a very important geodetic space technique. Impressive progress has been achieved for the mapping of the ocean surface, the kinematics of mean sea level, the gravity field of the Earth and Earth rotation. However a number of critical aspects for satellite altimetry remain and shall be indicated here.

The discussion on the correction for the inverse barometer response of the sea surface due to changes in atmospheric pressure is still controversy. The assumption that 1 hPa decrease in pressure causes an instantaneous sea level rise of 10mm (and vice versa) is violated for several reasons: the response is not instantaneous but more valid at longer time periods, it seems to be compensated at low latitude and there is a departure from observation at tide gauges. It is not clear what is the right average pressure to be used for the dry troposphere correction, 1013.3 or 1010.6 hPa (mean only over ocean surface) The difference implies a change of the mean sea surface of 2.7 cm. A dynamic baroclinic model should be used to determine the physically consistent sea level response to changes in atmospheric pressure.

The long-term stability is a critical issue for a well-founded statement about the global sea level rise. TOPEX/Poseidon is certainly exceptionally precise. But does it allow achieving the 1mm/year accuracy? This would imply that over a decade the global mean of sea surface heights are known with an accuracy of 10 mm! Nerem (1998) certifies a 2mm/year uncertainty in the long-term stability of TOPEX/Poseidon. There are uncertainties in most of the environmental corrections that exceed these requirements. Careful attention has also to be paid to the reference system and its stability (See Nerem et al. 1998, Ries et al. 1999). Reference system offset must be identified and taken into account, if long-term multi-mission altimetry is used to investigate secular sea level changes.

Most of the geodetic applications require a high spatial resolution. This can only be achieved by combining altimeter missions with different sampling characteristic. This combination requires a careful harmonisation of all missions and a dedicated cross-calibration in order to ensure a consistent vertical reference. The current situation with five altimeter missions operating simultaneously is extraordinary and must be used to perform an utmost precise cross-calibration of all missions. Only in this way a long-term record of altimetry can be generated. In a few years, however, there may be only a single mission, Jason-2.

Finally, geodesy has specific requirements to the precision of altimetry in coastal areas. Sea surface mapping and the recovery of gravity anomalies suffer from the degraded performance of coastal altimetry. Global tide models can not represent the shallow water tides. At the transition from land to sea there are fast changes in the atmosphere. A retracking is necessary to approach as close as possible to the coast.

7.2 The challenge of GRACE and GOCE

The geodetic and oceanographic community is waiting for dramatic improvements of the gravity field by analysing the data of CHAMP, GRACE and GOCE. All applications described above would essentially gain from these improvements. The specific expectations of geodesy focus on the realization of a cm-geoid. This will allow to

- unify national height systems,
- enable precise levelling with GPS,
- solve datum inconsistencies in terrestrial and marine gravity data, and - above all - to
- derive a precise estimate of the absolute dynamic topography with the perspective, to
  - get a detailed view of the surface currents, to
  - extrapolate surface currents to the deep ocean and to
  - obtain reliable estimates of heat and mass flux.

References

Acuña, G,. and W. Bosch (2003). Absolute Comparison of Satellite Altimetry and Tide Gauge Registrations in Venezuela, IAG Symposium, This Volume.

Acuña, G., W. Bosch and B. Meisel (2002). Correlation between Multi-Mission Altimeter Time Series and Tide Gauge Registrations in the Caribbean Sea, In IAG Symposium 124: Vertical Reference Systems, pp. 231-237, Springer-Verlag.

Anderson, O., P. Knudsen, S. Kenyon and R. Trimmer (2000). The KMS99 Global Marine Gravity Field – Improvements and Accuracy Assesment, EGS General Assembly, Nice.

Anderson, O., P. Knudsen and R. Trimmer (2001). The KMS2001 Global Mean Sea Surface and Gravity Field, Poster, IAG 2001 General Assembly, “Vistas For Geodesy In The New Millenium”, 2.-7. September 2001, Budapest, Ungary.

Anzenhofer, M., and T. Gruber (1995). MSS93A: A New Sationary Sea Surface Combining One Year Upgraded ERS-1 Fast Delivery Data and 1987 GEOSAT Altimeter Data, Bulletin Gèodèsique, 69, pp. 157-163.

Anzenhofer, M., T. Gruber and M. Rentsch (1996). Global High Resolution Mean Sea Surface Based on ERS-1 35- and 168-Day Cycles and TOPEX Data, International Association of Geodesy Symposia, 116, Global Gravity Field and Its Temporal Variations, Springer.

AVISO/Altimetry (1998). AVISO User Handbook, Corrected Sea Surface Heights (Corsshs), AVI-NT-011-311-CN, Edition 3.1.

AVISO (1999). Side B TOPEX Altimeter Evaluation, AVI-NT-011-317-CN, Edition 1.0.

Bosch, W. (1993). A Rigorous Least Squares Combination of Low and High Degree Spherical Harmonics, IAG General Meeting, Beijing, China.
Bosch, W. (1997). Goeid and Orbit Corrections from Crossover Satellite Altimetry, Report No. 63, Deutsches Geodätisches Forschunginstitut, München.
Bosch, W. (1999). Variations of Geocenter and Earth Orientation from Estimates of Ocean Mass Redistribution, The 22nd General Assembly of the IUGG.
Bosch, W., J. Klokočnik, C. A. Wagner and J. Kostelecký (2000). Geosat and ERS-1 Datum Offsets Relative to TOPEX/POSEIDON Estimated Simultaneously with Geopotential Corrections from Multi-Satellite Crossover Altimetry, In: Rummel R., H. Drewes, W.Bosch, H. Hornik (Eds.) Towards an Integrated Global Geodetic Observing System (IGGOS). IAG Section II Symposia, 120, Springer, pp. 96-98.
Bursa, M., J. Kouba, A. Müller, K. Radej, S. A. True, V. Vatrt and M. Vojtiskova (1999). Differences between Mean Sea Levels for the Pacific, Atlantic and Indian Ocean from TOPEX/POSEIDON Altimetry, Studia Geoph et Geod, 43, pp.1-6.
Bursa, M., S. Kenyon, J. Kouba, K. Radej, V. Vatrt, M. Vojtiskova and J. Simek (2002). World Height System Specified by Geopotential at Tide Gauge Stations, In: Drewes H., A. Doodson, L.P.S. Fortes, L. Sanchez, P. Sandoval (Eds.) Vertical Reference Systems. IAG Symposia, 124, Springer, pp. 291-296.
Cazenave, A., P. Schaeffer, M. Bergé, C. Brossier, K. Dominh, and M.C. Gennero (1996). High Resolution Mean Sea Surface Computed with Altimeter Data of ERS-1 and TOPEX-POSEIDON, Geophys J Int, 125, pp. 696-704.
Chambers, D., J. Ries, C. Shum and B. Tapley (1998). On the Use of Tide Gauges to Determine Altimeter Drift, J Geophys Res, 103, pp. 12885-12890.
Chelton, D. B., J. C. Ries, B. J. Haines, L. L. Fu and P. S. Callahan (2001). Satellite Altimetry, In: L.L. Fu and A. Cazenave (Eds.) Satellite Altimetry and Earth Sciences – A Handbook of Techniques and Applications. International Geophysical Series, 69, Academic Press, San Diego.
Chen, J. L., C. R. Wilson, R. J. Eanes and R. S. Nerem (1999). Mass Variations in the Earth System and Geocenter Motions, IERS Technical Note 25, Observatoire De Paris, Paris, pp. 27-36.
Christensen, E., et al. (1994). Calibration of TOPEX/POSEIDON at Platform Harvest, J Geophys Res, 99, pp. 24465-24485.
Dong, D., J. Dickey, Y. Chao and M. K. Cheng (1997). Geocenter Variations Caused by Atmosphere, Ocean and Surface Ground Water, Geophys Res Lett, 24, pp. 1867-1870.
Dong, X., P. Woodworth, P. Mooreand and R. Bingley (2002). Absolute Calibration of the TOPEX/POSEIDON Altimeters Using UK Tide Gauges, GPS, and Precise Local Geod-Differences, Mar Geod, 25, pp. 183-204.
Gross, R. (2002). Gravity, Oceanic Angular Momentum, and the Earth's Rotation, In: Sideris M.G. (Ed.) Gravity, Geoid and Geodynamics 2000. IAG Symposia, 123, Springer, pp. 153-158.
Gruber, T., A. Bode, C. Reigber, P. Schwintzer, G. Balmino, R. Biancale and J. M. Lemoine (2000). GRIM5-C1: Combination Solution of the Global Gravity Field to Degree and Order 120, Geophys Res Lett, 27, pp. 4005-4008.
Haxby, W. F., G. D. Karner, J. L. La Brecque and J. K. Weissel (1983). Digital Images of Combined Oceanic and Continental Data Sets and Their Use in Tectonic Studies, EOS Trans, 64, pp. 995-1004.
Hernandez, F., and P. Schaeffer (2001). The CLS01 Mean Sea Surface: A Validation with the GSFC00 Surface in Press, CLS Ramonville St Agne, France.
Heiskanen, W. A., and H. Moritz (1967). Physical Geodesy, W.H. Freeman and Company, San Francisco.
Imel, D. (1994). Evaluation of the TOPEX/POSEIDON Dual-Frequency Ionospheric Correction, J Geophys Res, 99, pp. 24895-24906.
Kaula, W. M. (1966). Theory of Satellite Geodesy – Application of Satellites to Geodesy, Blaisdell Publishing Company, Waltham, Massachusetts.
Klokočnik, J., and C. A. Wagner (1999). Combinations of Satellite Crossovers to Study Orbit and Residual Errors in Altimetry. Celestial Mechanics and Dynamical Astronomy, 74, pp. 231-242.
Klokočnik, J., C. A. Wagner and J. Kostelecký (1996). Accuracy Assessment of Recent Earth Gravity Models Using Crossover Altimetry, Studia Geop et Geod, 40, pp. 77-110.
Klokočnik, J., C. A. Wagner and J. Kostelecký (1999). Spectral Accuracy of JGM3 from Satellite Crossover Altimetry, J Geod, 73, pp. 138-146
Koblinsky, et al. (1999a). NASA Ocean Altimeter Pathfinder Project, Report 1: Data Processing Handbook, NASA/TM-1998-208605.
Koblinsky, et al. (1999b). NASA Ocean Altimeter Pathfinder Project, Report 2: Data Set Validation, NASA/TM-1998-209230.
Laxon, S. W., and D. Mcadoo (1994). Arctic Ocean Gravity Field Derived from ERS-1 Satellite Altimetry, Science, 256, pp. 621-624.
Le Traon, P. Y., and F. Ogor (1998). ERS-1/2 Orbit Improvement Using TOPEX/POSEIDON: The 2 cm Challenge, J Geophys Res, 103, pp. 8045-8057.
Lemoine, F., et al. (1997). The Development of the Joint NASA GSFC and the National Imagery and Mapping Agenvcy (NIMA) Geopotential Model EGM96, NASA/TP-1998-206861, Goddard Space Flight Centre, Greenbelt.
Levitus, S., T. Boyer and R. Bugett (1994). World Ocean Atlas 1994 (WOA94), NOAA Atlas NESDIS, U.S. Department Of Commerce, Washington D.C.
Mcadoo, D. C., and K. M. Marks (1992a). Resolving Marine Gravity with ERS-1 Satellite Altimetry, Geophys Res Letters, 19, pp. 2271-2274.
Mcadoo, D. C., and K. M. Marks (1992b). Gravity Field of the Southern Ocean from Geosat Data, J Geophys Res, 97, pp. 3247-3260.
Mitchum, G. T. (1994). Comparison of TOPEX Sea Surface Heights and Tide Gauge Sea Levels, J. Geophys. Res., Vol. 99(C12), pp. 24541-24553.
Mitchum, G. T. (1998). Monitoring the Stability of Satellite Altimeters with Tide Gauges, J Atmos Ocean Tech, 15, pp. 721-730.
Mitchum, G. T. (2000). An Improved Calibartion of Satellite Altimetric Heights Using Tide Gauge Sea Levels with Adjustment For Land Motion, Mar Geod, 23, pp. 145-166.
Neilan, R., P. A. Van Scoy and P. L. Woodworth (1998). GPS and Tide Gauge Benchmark Monitoring and GPS Altimeter Calibration. Proceedings of the Workshop on Methods for Monitoring Sea Level, IGS-PSMSL, IGS Central Bureau, Pasadena, California, U.S.A.
Nerem, R., R. Eanes, J. Riesand and G. Mitchum (1998). The Use of a Precise Reference Frame in Sea Level Change Studies, In: IAG Symposium 120, Towards an Integrated Global Geodetic Observing System (IGGOS), pp. 8-12, Springer-Verlag.
Ries, J., R. Eanes and R. Nerem (1999). The ITRF97 Reference Frame and Its Effect on Sea Level Change Studies, TOPEX/POSEIDON and JASON-1 Science Working Team 1999 Meeting, October 25-27.
Rummel, R., and R. Haagmanns (1991). Gravity Gradients from Satellite Altimetry, Mar Geod, 14, pp. 1-12.

Rosborough, G. W. (1986). Satellite Orbit Pertubations Du to the Geopotential, CSR-86-1, Univ. of Texas at Austin, Cente for Space Research.
Sandwell, D. T., and W. H. F. Smith (1997). Marine Gravity from Geosat and ERS-1 Satellite Altimetry, J Geophys Res, 102, pp. 10039-10054.
Scharro, R., and P. N. A. M. Visser (1998). Precise Orbit Determination and Gravity Field Improvement for the ERS Satellites, J Geophys Res, 103, pp. 8113-8127.
Schuh, W. D. (1996). Tailored Numerical Solution Strategies for the Global Determination of the Earth Gravity Field, Techn Report, Inst. Theor. Geod., Techn Univ. Graz, Austria.
Schrama, E. J. O. (1989). The Role of Orbit Errors in Processing of Satellite Altimeter Data, The Netherlands Geodetic Commission. Publication on Geodesy, No. 33, Delft.
Shum, C. K., B. H. Zang, B. E. Schutz and B. D. Tapley (1990). Altimeter Crossover Methods for Precision Orbit Determination and the Mapping of Geophysical Parameters, J Astron Sci, 38, pp. 355-368.
Semtner, A. J., and R. M. Chervin (1992). Ocean Circulation from a Global Eddy-Resolving Model, J Geophys Res, 97, pp. 5493-5550.
Smith, W., and D. Sandwell (1997). Global Seafloor Topography from Satellite Altimetry and Ship Depth Soundings, Science, 277, pp. 1956-1961.
Stammer, D., C. Wunsch, R. Giering, C. Eckert, P. Heimbach, J. Marotzke, A. Adcroft, C. N. Hill and J. Marshall (2003). Volume, Heat and Freshwater Transports of the Global Ocean Circulation 1993--2000, Estimated from a General Circulation Model Constrained by World Ocean Circulation Experiment (WOCE) Data, J Geophys Res, 108, 3007.
Wang, Y. M. (2001). GSFC00 Mean Sea Surface, Anomaly and Vertical Gravity Gradient from Satellite Altimeter Data, J Geophys Res, 106, pp. 31167-31174.
Wagner, C., and J. Klokocnik (1995). The Role of Geodetic Errors in Connecting Ocean Surfaces over Disparate Satellite Altimeter Missions, IUGG GA Boulder.
Wagner, C. A., J. Klokocnik and R. Cheney (1997). Making the Connection between Geosat and TOPEX/POSEIDON, J Geod, 71, pp. 273-281.
Wahr, J., M. Molenaar and F. Bryan (1998). Time Variability of the Earth's Gravity Field: Hydrological and Oceanic Effects and Their Possible Detection Using GRACE, J Geophys Res, 103, pp. 30205-30229.
Wunsch, C., and D. Stammer (2003). Global Ocean Data Assimilation and Geoid Measurements, Space Sci Rev, In Press.
Yunck, T. P., W. I. Bertiger, S. C. Wu, Y. Bar-Sever, E. J. Christensen, B. J. Haines, S. M. Lichten, R. J. Muellerschoen, Y. Vigue and P. Willis (1994). First Assessment of GPS-Based Reduced Dynamic Orbit Determination on TOPEX/POSEIDON, Geophy Res Lett, 21, pp. 541-544.
Yi, Y. (1995). Determination of Gridded Mean Sea Surface from TOPEX, ERS-1, and GEOSAT Altimeter Data, Rep. 434, Dept. Geod. Sci.Surv., The Ohio State Univ., Colombus, USA.